CHAPTER - IV

MICROCOMPUTER BASED MEASUREMENTS OF HARMONICS AND ESTIMATION OF AUTO-CORRELATION IN ELECTRICAL NETWORKS

CHAPTER IV

MICROCOMPUTER BASED MEASUREMENTS OF HARMONICS AND ESTIMATION OF AUTOCORRELATION IN ELECTRICAL NETWORKS

4.1.1. INTRODUCTION

Proliferation of electronic control of equipments by semiconductor devies (SCRs and Thyristors) generates harmonics in the electricity supply network. These harmonics of 50 (60) Hz range from audible frequencies into the radio frequencies of 1 MHz and beyond may affect unfavorably the operation of other electrical or electronic equipment connected to the same electricity supply network. 'Network pollution' by harmonics has now been added to ecological, biological, atmospheric, etc. pollution, and a need arises to limit harmonic currents and voltages in distribution networks.

4.1.2. VOLTAGE DISTORTION

'Total harmonic voltage distortion' is expressed as a percentage of the fundamental, namely,

$$U_T = 100 \frac{\sqrt{\sum_{N=2}^{\infty} U_N^2}}{U_o}$$

where

U_T = percentage of total harmonic voltage distortion

N = order number of harmonic (second, third, etc.), (normally $2 < N < 40$)

U_N = voltage of each individual harmonic

U_o = voltage of the (50/60 Hz) fundamental.

Voltage distortion at frequencies close to a harmonic frequency (that is so-called 'noncharacteristic harmonics') should be treated in a similar fashion to that of the closest conventional frequency, in which N is a whole number (integer).

4.1.3. HARMONIC GENERATION

A distribution network can be considered to consist of a series of network impedence connected in series. Any harmonic currents flowing in the system which can be considered in terms of Fourier analysis to be a combination of d.c. and sine and cosine waves at various amplitudes and frequencies will create, therefore, appropriate voltage drops across the various network impedences in terms of Ohm's law. The result will be voltage wave distortion, which will be more pronounced in the vicinity of the distortion-producing device than they will be further away in the

network. This means that a consumer close to the harmonics source will be more affected than a consumer who is both physically and electrically more remote from it. In term of Fourier analysis, there is theoretically no limit to the frequencies which could be generated by various periodic wave shapes. In theory at least, one could face from pure d.c. right through the whole audio range up into high frequencies of medium and even short radio waves. Fortunately, however, the practical situation is not quite as drastic as this appear to be.

Since proliferation of electronic control of equipments by semiconductor devices generate harmonics in the electricity supply network, every major industrial process is therefore subject to the presence of harmonics. These devices inherently display a poor power factor which in turn may create a parallel resonant condition with the utility source for harmonic required by the load - perhaps the worst effect of excessive harmonics. Therefore with the complexity of modern installations it is essential for a user to have a harmonic study performed in most instances. To determine whether or not a voltage distortion level would be excluded, a harmonic analysis study is necessary for a new installation, alternatively field testing may be performed for existing power systems.

4.2.1. HARMONIC ESTIMATION SIGNAL MODEL

A general model of voltage and current signals, during abnormal conditions, in electrical networks contain a decaying d.c. component plus higher order harmonics, has been chosen for estimation of different harmonic contents in the signal.

The signal model is

$$y(t) = \sum_{n=1}^{N} (\alpha_n \cos n\omega_o t + \beta_n \sin n\omega_o t) + a_o e^{-\tau t} \qquad (4.1)$$

where

$y(t)$ = Instantaneous differential current or voltage samples at time t.

α_n, β_n = Functions of Fourier coefficients.

a_o = dc component.

τ = Decaying time constant of the dc component.

N = Harmonic number of the highest frequency present in the signal $y(t)$.

ω_o = $2\pi/T$, T is the period of the function.

The d.c. term in the equation (4.1) can be expanded and the equation can be rewritten as

$$y(t) = \sum_{n=1}^{N} (\alpha_n \cos n\omega_o t + \beta_n \sin n\omega_o t) + a_o'' t^2 + a_o' t + a_o \qquad (4.2)$$

For estimation of different harmonics in the signal, the α's and β's are to be determined. Discrete Fourier transform may be viewed as the determination of the coefficients α_1 , α_2 .... α_n , β_1 , β_2 .... β_n and a_o'' , a_o' and a_o.

The determination of these functions of Fourier coefficients are done by two algorithms.

(1) Spectral observer

(2) Recursive functional expansion.

4.2.2. SPECTRAL OBSERVER (ALGORITHM NO.1)

For the harmonic signal model (4.2), a convinient state variable model is the following :

$$\dot{x} = \begin{bmatrix} \dot{x}_1 \\ \dot{x}_2 \\ \vdots \\ \dot{x}_{2N-1} \\ \dot{x}_{2N} \\ \dot{x}_{2N+1} \\ \dot{x}_{2N+2} \\ \dot{x}_{2N+3} \end{bmatrix} = \begin{bmatrix} 0 & 1 & & & & & & \\ -\omega_o^2 & 0 & & & & & & \\ & & \ddots & & & & & \\ & & & 0 & 1 & 0 & 0 & 0 \\ & & & -(N\omega_o)^2 & 0 & 0 & 0 & 0 \\ & & & 0 & 0 & 0 & 0 & 0 \\ & & & 0 & 0 & 0 & 0 & 1 \\ & & & 0 & 0 & 0 & 1 & 0 \end{bmatrix} \begin{bmatrix} x_1 \\ x_2 \\ \vdots \\ x_{2N-1} \\ x_{2N} \\ x_{2N+1} \\ x_{2N+2} \\ x_{2N+3} \end{bmatrix}$$

$$\dot{x} = Ax \qquad (4.3)$$

$$y = C^T x \qquad C^T = [1\ 0\ 1\ 0 \ldots\ldots 1\ 0\ 1\ 0\ 0]$$

In this form of the state equations, constants and each harmonic term in the response are decoupled from one another. Although the bandlimited periodic signal $y(t)$ may not actually be produced by the system (4.2), it may be considered to be the output of the system.

For the continuous-time signal $y(t)$ a discrete-time system of the form

$$\begin{aligned} \epsilon(k+1) &= \exp(A\Delta t)\ \epsilon(k) \\ &= \phi\, \epsilon(k) \\ y(k) &= C^T\ \epsilon(k) \end{aligned} \tag{4.4}$$

produces samples of the corresponding continuous time system (4.3) signals with sampling interval Δt. ϕ is the state transition matrix and C is the output coupling matrix. In particular

$$\epsilon(k) = x(k\Delta t).$$

To observe this model, the related nth order related system of the type

$$\begin{aligned} \xi(k+1) &= \phi\,\xi(k) + g[y(k\Delta t) - C^T \xi(k)] \\ &= (\phi - gC^T)\,\xi(k) + g\, y(k\Delta t) \\ \gamma(k) &= C^T \xi(k) \end{aligned} \tag{4.5}$$

is termed as an identity observer [13] - [19] for the system (4.4).

Here

$$\phi = \begin{bmatrix} \phi_1 & \\ & \phi_d \end{bmatrix} = \exp(A\Delta t) \qquad (4.6)$$

$$\phi_1 = \text{block diag} \begin{bmatrix} \cos i\omega_o\Delta t & \frac{\sin i\omega_o\Delta t}{i\omega_o} \\ -i\omega_o \sin i\omega_o\Delta t & \cos i\omega_o\Delta t \end{bmatrix}$$

$$i = 1, 2, \ldots\ldots, N$$

$$\phi_d = \begin{bmatrix} \frac{1}{2}\Delta t^2 & \Delta t & 1 \\ 0 & \Delta t & 1 \\ 0 & 0 & 1 \end{bmatrix}$$

and $\omega_o\Delta t = \frac{2\pi}{N_s}$, N_s is no. of samples per cycle of the waveform.

Over the years many methods of calculating the observer gain vector g for a given system and the desired observer eigenvalues have been developed [15 , 16, ...]. For Nyquist rate spectral observer, a simple observer gain calculation may be used [15]. For our purpose the value of g may be chosen as :

$$g = \frac{1}{2N+1} [\cos 2N\omega_o\Delta t \; , \; \omega_o \sin 2N\omega_o\Delta t \ldots\ldots$$
$$\ldots\ldots \cos 2N.N\omega_o\Delta t \; \sin 2N.N\omega_o\Delta t \; ,$$
$$3\Delta t^2 \; , \; -\frac{5}{2}\Delta t \; , \; 1] \qquad (4.7)$$

However, for any sampling rate other than the Nyquist rate, a general method of gain calculation is given in Appendix I.

For a given sampling rate and data window, the gain vector g is calculated in advance of signal processing and spectral observer computation assume the simplified form

$$\xi_i(k+1) = a_i \xi_i(k) + b_i \xi_{i+1}(k) + g_i[y(k\Delta t) - \gamma(k)] \qquad i = 1,3,5,\ldots\ldots,2N-1 \tag{4.8}$$

$$\xi_i(k+1) = d_i \xi_{i-1}(k) + a_i \xi_i(k) + g_i[y(k\Delta t) - \gamma(k)] \qquad i = 2,4,6,\ldots\ldots,2N \tag{4.9}$$

$$\xi_{2N+1}(k+1) = \xi_{2N+1}(k) + \Delta t\, \xi_{2N+2}(k) + \tfrac{1}{2}\Delta t^2 \xi_{2N+3}(k) + g_{2N+1}[y(k\Delta t) - \gamma(k)] \tag{4.10}$$

$$\xi_{2N+2}(k+1) = \xi_{2N+2}(k) + \Delta t\, \xi_{2N+3}(k) + g_{2N+2}[y(k\Delta t) - \gamma(k)] \tag{4.11}$$

$$\xi_{2N+3}(k+1) = \xi_{2N+3}(k) + g_{2N+3}[y(k\Delta t) - \gamma(k)] \tag{4.12}$$

$$\gamma(k) = \xi_1(k) + \xi_3(k) + \ldots\ldots + \xi_{2N+1}(k) \tag{4.13}$$

In the above equations, the vector a , b and d are defined (which are computed in advance of signal processing) as :

$$a^T = [\cos \omega_o \Delta t \quad \cos 2\omega_o \Delta t \ldots\ldots \cos N\omega_o \Delta t]$$

$$b^T = [\frac{\sin \omega_o \Delta t}{\omega_o} \quad \frac{\sin 2\omega_o \Delta t}{2\omega_o} \ldots\ldots \frac{\sin N\omega_o \Delta t}{N\omega_o}] \qquad (4.14)$$

$$d^T = [-\omega_o \sin \omega_o \Delta t \quad -2\omega_o \sin 2\omega_o \Delta t \ldots -N\omega_o \sin N\omega_o \Delta t]$$

For harmonic estimation only the α's and β's are to be determined for which the equations (4.8) and (4.9) are to be solved iteratively to yield the coeffic ients.

$$\alpha_1 = \xi_1 , \alpha_2 = \xi_3 , \ldots\ldots, \alpha_N = \xi_{2N-1}$$
$$\beta_1 = \xi_2/\omega_o , \quad \beta_2 = \xi_4/2\omega_o \ldots\ldots, \beta_N = \xi_{2N}/N\omega_o \qquad (4.15)$$

From this the value of fundamental, second, third and so on harmonics components can be obtained as

$$I^2_{fund} = \xi_1^2 + (\xi_2/\omega_o)^2 , \quad I^2_{second} = \xi_3^2 + (\xi_4/2\omega_o)^2$$
$$I^2_{third} = \xi_5^2 + (\xi_6/3\omega_o)^2 \ldots\ldots\ldots \qquad (4.16)$$

4.2.3. RECURSIVE FUNCTIONAL EXPANSION (ALGORITHM NO.2)

Another approach for measurement of harmonic contents in a signal, by generating recursive Fourier transform from a sequence of signal samples y(k) , is by the use of functional expansion, a concept commonly used in digital signal

processing and control theory. The most familiar applications of discrete linear transforms involves Fourier expansion of the signal model.

The discrete linear transform of data samples $y(k)$ can be represented on the basis of basis function f_1 as

$$y(k) = \sum_{i=1}^{n} X(i)\, f_i(k)$$

$$k = 0,1,\ldots,\ n-1 \qquad (4.17)$$

The above equation can generate the transform solution of the X vector in recursive manner.

If we consider the signal to be represented by equation (4.2), then the choice of the basis function would be

$$D(k) = \begin{bmatrix} f_1 = \cos Lk \\ f_2 = \sin Lk \\ \vdots \\ f_{2N-1} = \cos NLk \\ f_{2N} = \sin NLk \\ f_{2N+1} = 1 \\ f_{2N+2} = kt \\ f_{2N+3} = (kt)^2 \end{bmatrix} \qquad (4.18)$$

where L is a positive constant.

For Nyquist rate of sampling

$$L = \frac{2\pi}{2N+3}$$

For sample rates other than Nyquist rate

$$L = \frac{2\pi}{N_s}$$

where N_s is the number of samples per period of the wave form.

When $L = 2\pi/N_s$, then this choice of basis function results in functional expansion of $y(k)$ as

$$\begin{aligned} y(k) &= X(1)\cos\frac{2\pi k}{N_s} + X(2)\sin\frac{2\pi k}{N_s} + \ldots. \\ &+ X(2N-1)\cos\frac{2\pi Nk}{N_s} + X(2N)\sin\frac{2\pi Nk}{N_s} \\ &+ X(2N+1) + X(2N+2)\,kt + X(2N+3)\,(kt)^2 \end{aligned} \tag{4.19}$$

From the above expression the Fourier coefficients can be determined as

$$\begin{aligned} \alpha_1 &= X(1), \quad \alpha_2 = X(3), \ldots, \alpha_N = X(2N-1) \\ \beta_1 &= X(2), \quad \beta_2 = X(4), \ldots, \beta_N = X(2N) \end{aligned} \tag{4.20}$$

and the value of the fundamental, second, third and so on harmonic contents in the signal can be calculated as

$$\begin{aligned} I^2_{fund} &= X^2(1) + X^2(2), \quad I^2_{second} = X^2(3) + X^2(4) \\ I^2_{3rd} &= X^2(5) + X(6)^2 \ldots I^2_{Nth} = X^2(2N-1) + X^2(2N) \end{aligned} \tag{4.21}$$

4.3. HARMONIC ESTIMATION OF MAGNETZING INRUSH CURRENTS OF A TRANSFORMER AND ELECTRICAL TRANSMISSION NETWORK UNDER FAULT CONDITION

A typical example for testing the algorithms is the case of a circuit element like a transformer which draws a large magnetizing current from the supply comprising of a d.c. offset and a large number of even and odd harmonic components during switching condition. Out of these the second harmonic is significant and is sometimes upto 20 % of the fundamental, and also third and fifth harmonic components are present to some extent. In certain cases of CT saturation and over excitation of transformers significant amount of 3rd and 5th harmonic currents are found. A short circuit on the primary or secondary side of the transformer also causes the current drawn from the supply to be non-sinusoidal. Unlike the magnetizing inrush case, the second harmonic in this case is much smaller i.e. < 15 % of the fundamental component. The d.c. component is found to be smaller also.

Both the algorithms are used to compute the harmonic components of transformer current. The estimation of harmonics in a power transmission network under fault condition has been studied in real-time using both the algorithms.

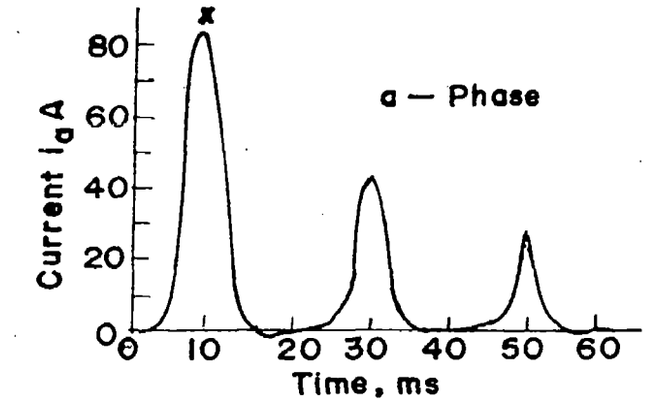

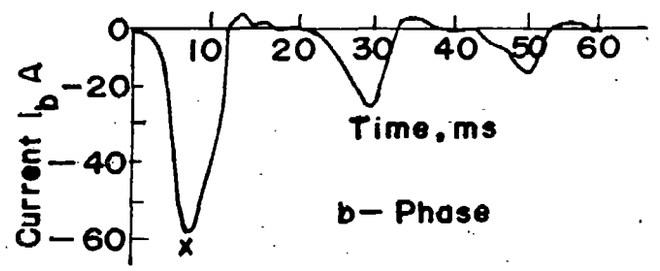

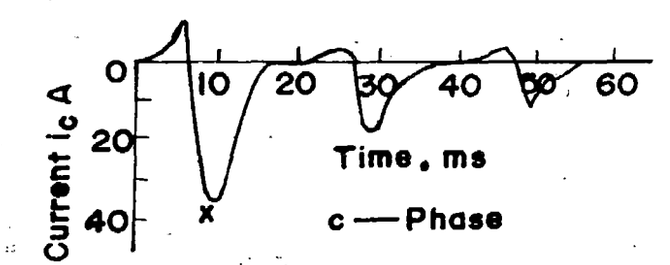

(a) Wire supply, secondary on open circuit

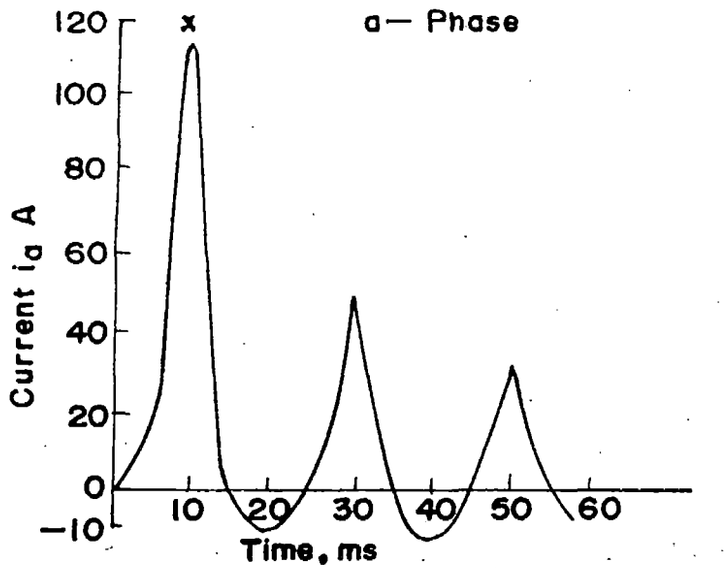

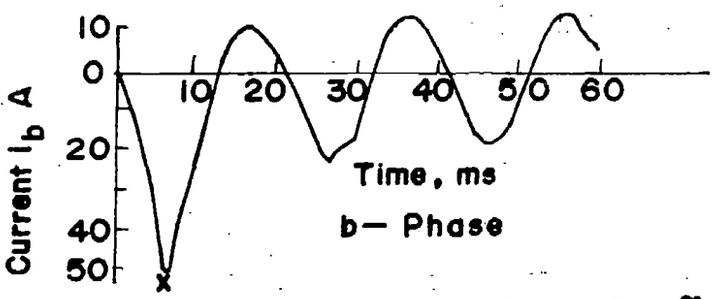

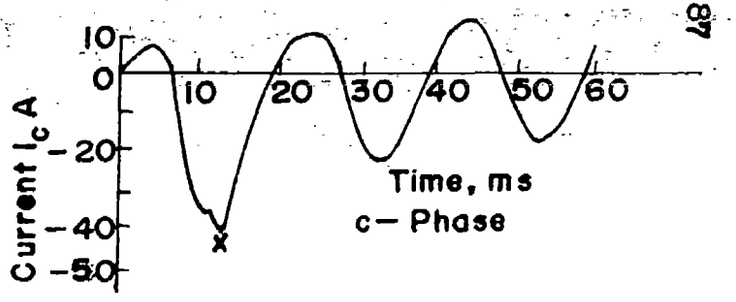

(b) Wire supply, secondary in loaded condition

Fig. 4.1 Inrush current wave form in Transformer

4.4. TEST RESULTS

For estimation and detection of harmonics the datas from a 415 V , 4 KVA, 3-phase transformer during open circuit and loading conditions and power transmission circuit at fault condition have been implemented in an LSI-11/23 16-bit microcomputer.

4.4.1. HARMONIC ESTIMATION IN TRANSFORMER

Fig. 4.1 shows the magnetizing inrush current waveform, of a 3-phase transformer, for a and b phases during open-circuit and loading condition.

Figs. 4.2 and 4.3 show the harmonic contents of the magnetizing inrush currents in real-time. From Figs. 4.2(a) and 4.2(b), it is evident that the relative magnitudes of fundamental, 2nd, 3rd harmonic components are different for a and b phases of the transformer during open-circuit condition. The second harmonic component is found to be substantial and can be used for relaying and instrumentation purposes. However 3rd harmonic component of the current can be used for the prediction of the saturation and over excitation conditions of the transformer. Similar situations are shown in Figs. 4.3(a) and 4.3(b) for loaded condition of the transformer. The data for the above estimation are given Table No. 4.1.

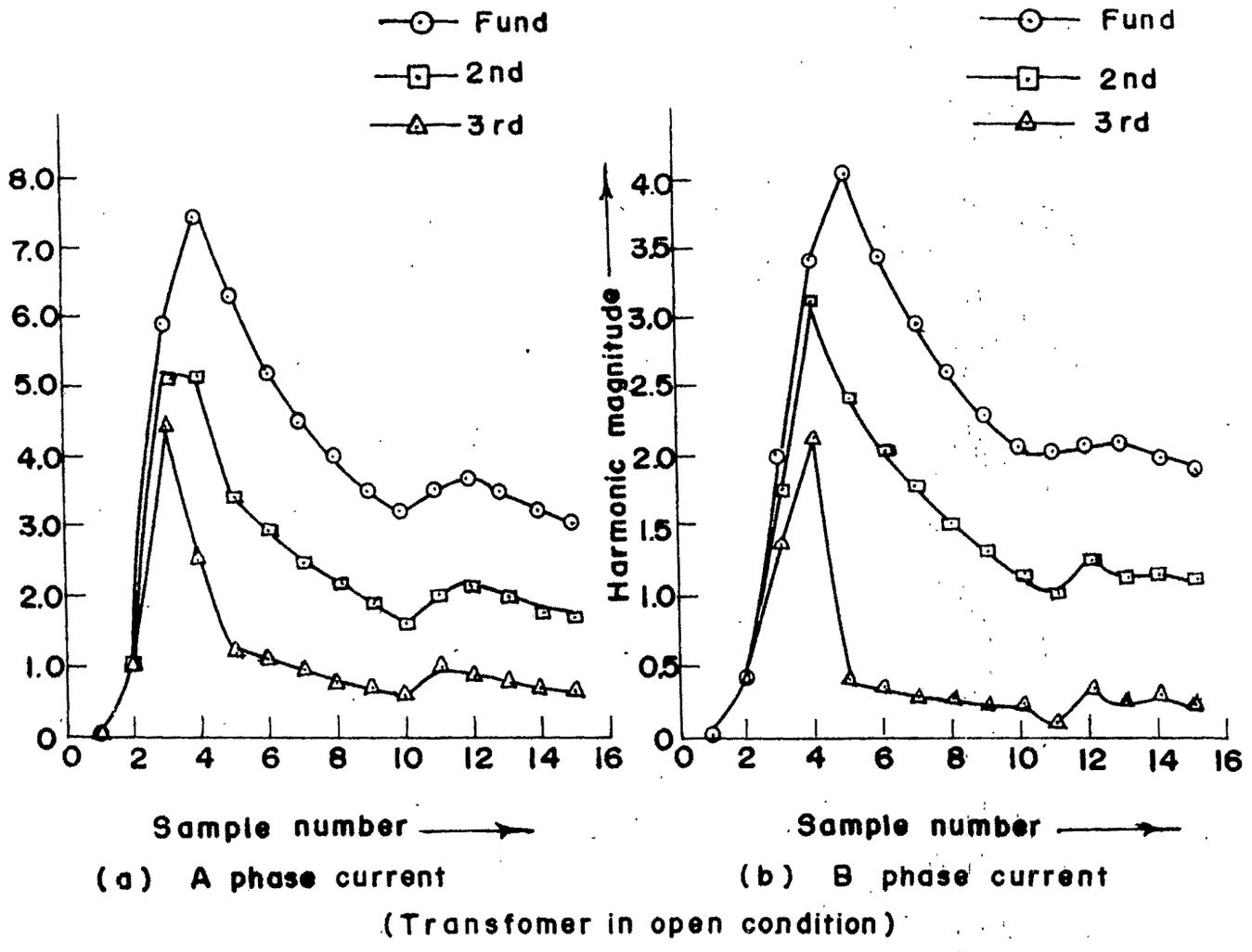

Fig. 4.2 Estimation of harmonics for magnitizing inrush currents

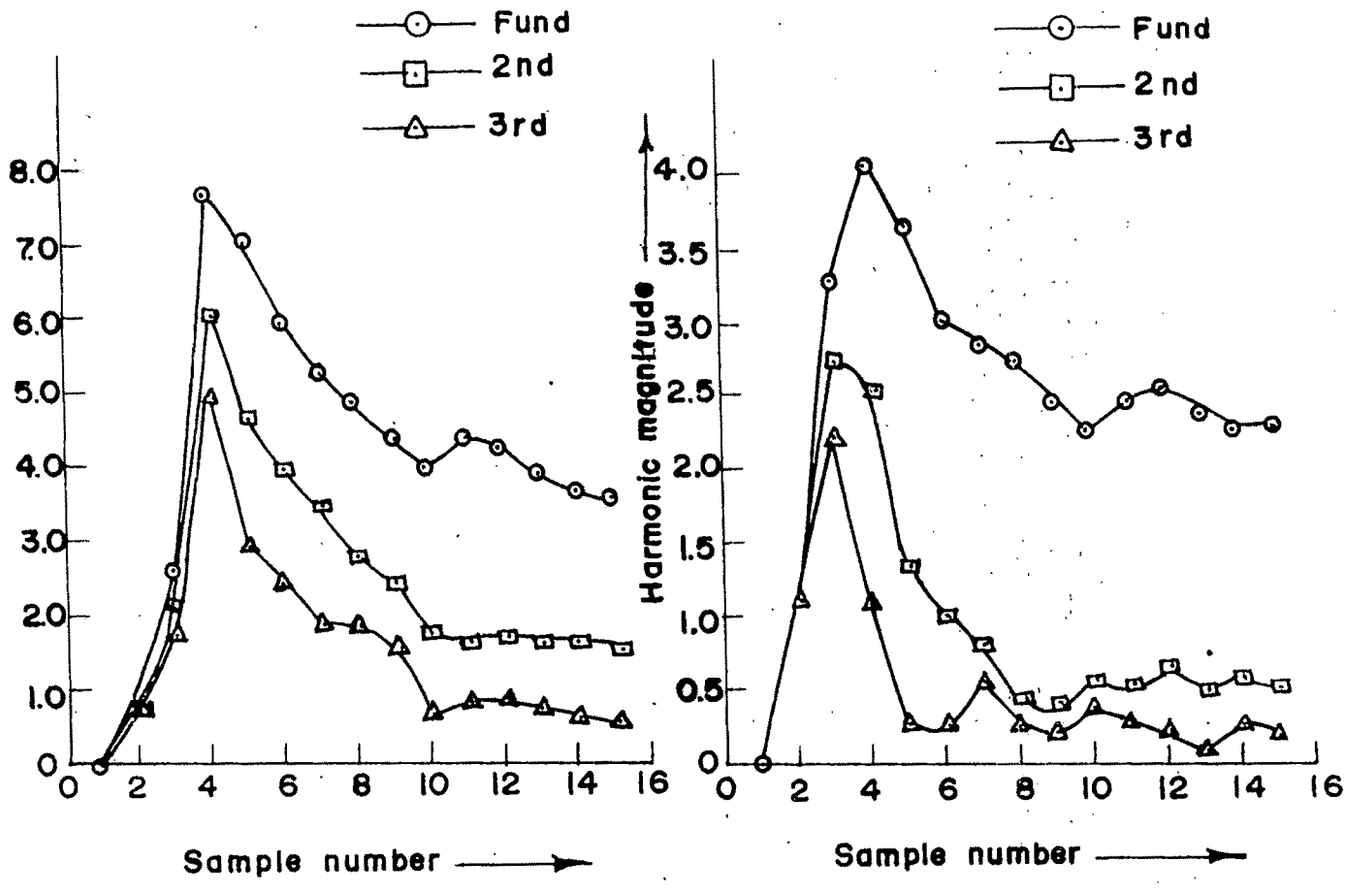

(a) A-phase current (b) B-phase current

(Transformer in loading condition)

Fig. 4.3 Estimation of harmonics for magnetizing inrush current

TABLE No.4.1(a)

Transfermer Open Condition A - PHASE CURRENT

	Signal magnitude	Fund	2nd	3rd
1	1.100	0.000	0.000	0.000
2	8.00	1.10	1.10	1.100
3	7.80	5.8748	5.3836	4.8427
4	2.10	7.5291	5.2178	2.5183
5	0.14	6.338	3.3713	1.2570
6	-0.14	5.2663	2.9412	1.0931
7	0.00	4.5499	2.4945	0.9596
8	0.00	3.9812	2.1827	.8396
9	0.45	3.5388	1.9402	.7463
10	3.25	3.2156	1.6795	.5832
11	3.45	3.4703	1.9792	.9896
12	0.50	3.7113	2.1896	.9062
13	0.15	3.4578	1.9693	.7685
14	0.00	3.2037	1.8126	.7342
15	0.00	2.9901	1.6918	.6833

TABLE No.4.1(b)

Transformer Open Condition B - PHASE CURRENT

Sl. No.	Signal magnitude	Fund	2nd	3rd
1	0.40	0.000	0.000	0.000
2	-2.65	.400	.400	.400
3	-5.50	1.9593	1.7867	1.4643
4	-3.90	3.7599	3.2340	2.1403
5	.20	4.0851	2.4126	.3980
6	.16	3.3965	2.0758	.3687
7	.12	2.9402	1.7890	.2707
8	.00	2.6025	1.5362	.2614
9	- .30	2.3134	1.3655	.2324
10	- .80	2.0773	1.1706	.2471
11	-1.80	1.9874	1.0387	.0792
12	-1.55	2.1218	1.2508	.3553
13	.35	2.1352	1.1480	.2662
14	.35	1.9789	1.1605	.2892
15	.15	1.8782	1.0965	.2252

TABLE No.4.1(c)

Transformer Loading Condition A - PHASE CURRENT

Sl. No.	Signal Magnitude	Fund	2nd	3rd
1	.80	0.000	0.000	0.000
2	3.45	.800	.800	.800
3	12.55	2.7036	2.3611	1.9596
4	4.00	7.6679	6.1232	5.1214
5	- .25	7.1292	4.7054	2.9516
6	-1.10	5.9435	4.0044	2.4745
7	-1.00	5.3290	3.4611	1.8680
8	.00	4.9122	2.7810	1.8834
9	2.20	4.3664	2.4720	1.6066
10	5.20	3.9861	1.7909	.7111
11	1.40	4.4353	1.7248	.8815
12	- .40	4.2889	1.7996	.8641
13	-1.30	3.9400	1.6824	.7877
14	-1.05	3.7087	1.7367	.6396
15	- .40	3.5888	1.5811	.6025

TABLE No.4.1(d)

Transformer Loading Condition B - PHASE CURRENT

Sl. No.	Signal Magnitude	Fund	2nd	3rd
1	-1.10	0.000	0.000	0.000
2	-4.15	1.100	1.100	1.100
3	-4.10	3.3259	2.8623	2.3072
4	-2.60	4.0547	2.5606	1.0869
5	- .30	3.6564	1.3510	.2690
6	1.10	3.0245	1.0380	.2450
7	1.05	2.8613	.7823	.5157
8	0.00	2.7575	.4278	.2548
9	-1.02	2.4511	.3803	.1807
10	-2.40	2.2641	.5549	.4968
11	-2.00	2.4580	.5305	.2924
12	- .80	2.5623	.6464	.2090
13	1.20	2.4188	.5131	.0946
14	1.60	2.3044	.6207	.2818
15	1.35	2.3485	.5144	.2304

4.4.2. Harmonic Estimation in Electrical Transmission Network

Another important example is the estimation of harmonics in a power transmission circuit under fault conditions. The data samples are the same as presented in Chapter V (Table No.5.2). Fig. 4.4 shows the estimation of fundamental, 2nd, 3rd and 5th harmonic components of the fault voltage. After recursive computation for a cycle (12 samples) the phase voltage become almost steady and is nearly 1.4 per unit. However after the onset of a fault on the 13th sample, the voltage magnitude changes and falls down and the magnitude of harmonics change and finally after stabilization is attained, the magnitudes become very small. Similar situations for line currents are shown in Fig. 4.5. As the fault in unbalanced all possible harmonics are generated.

Figs. 4.6 and 4.7 show the computation of the voltage and current harmonics using a spectral observation technique for an electrical transmission network.The results reveal the relative magnitudes of fundamental and harmonic components before and after the onset of the fault on the transmission system.

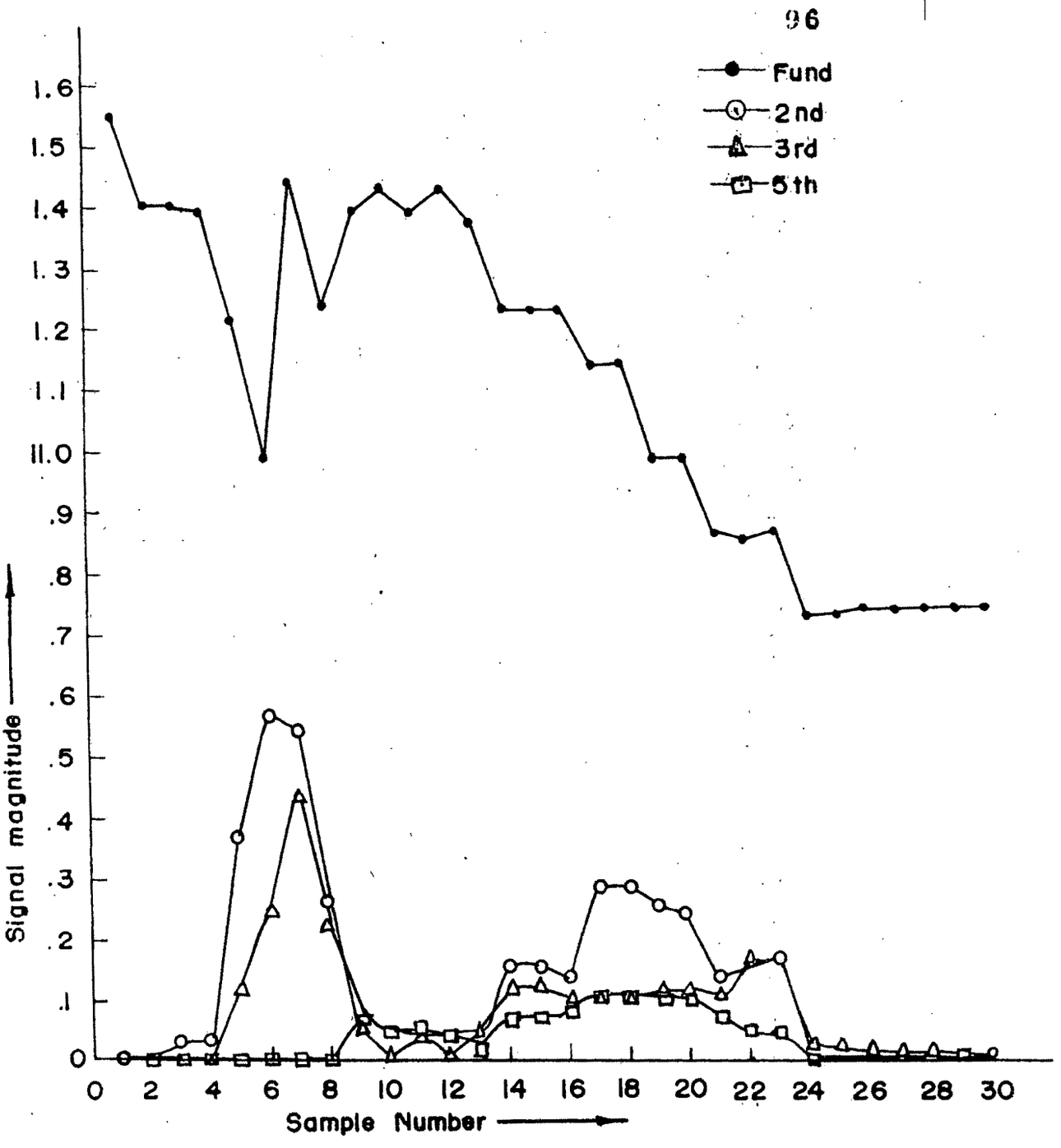

Fig. 4.4 Harmonic estimation of voltage in electrical transmission network using functional expansion

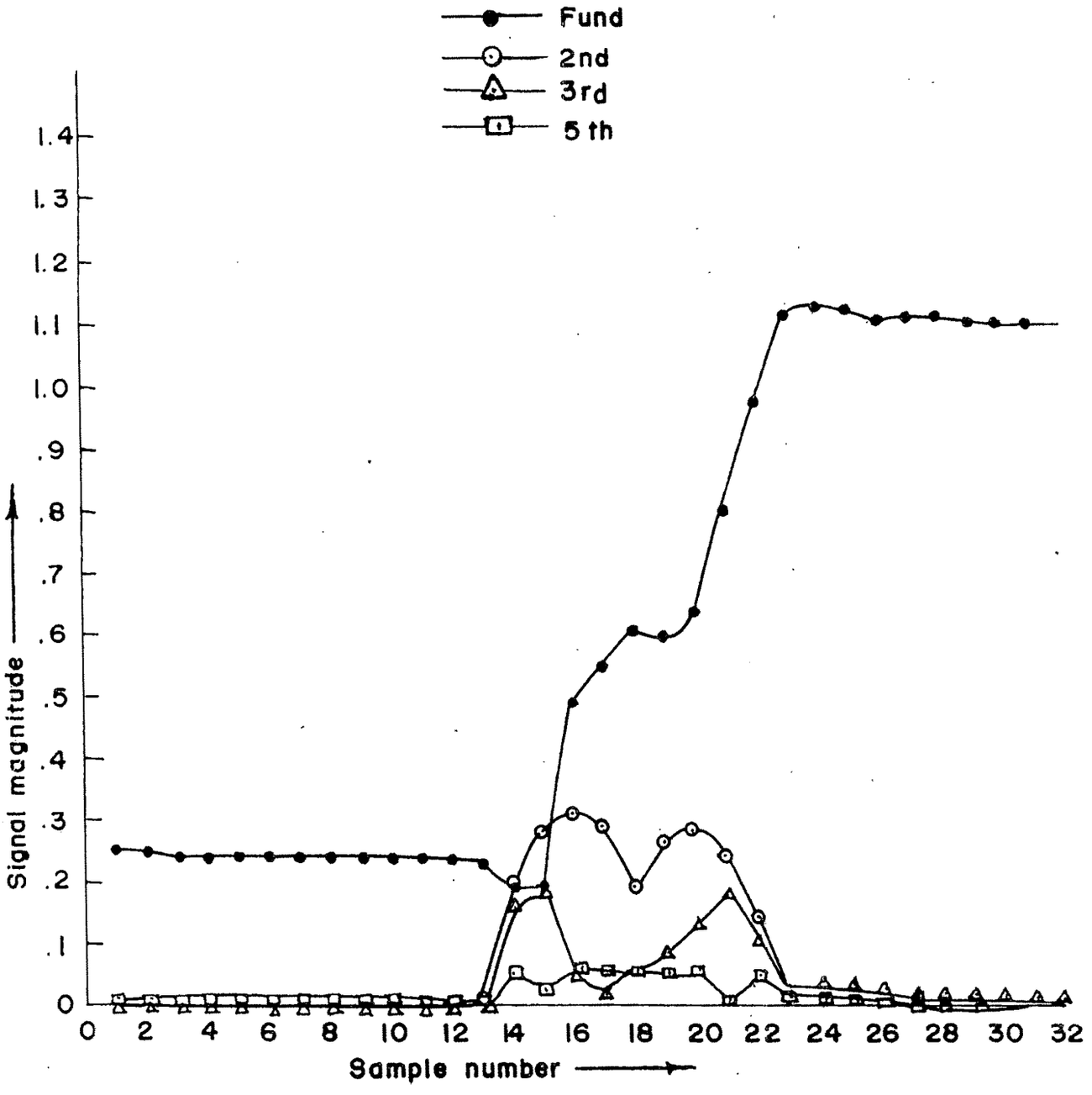

Fig. 4.5 Harmonic estimaton of current in electrical transmission network using functional expansion

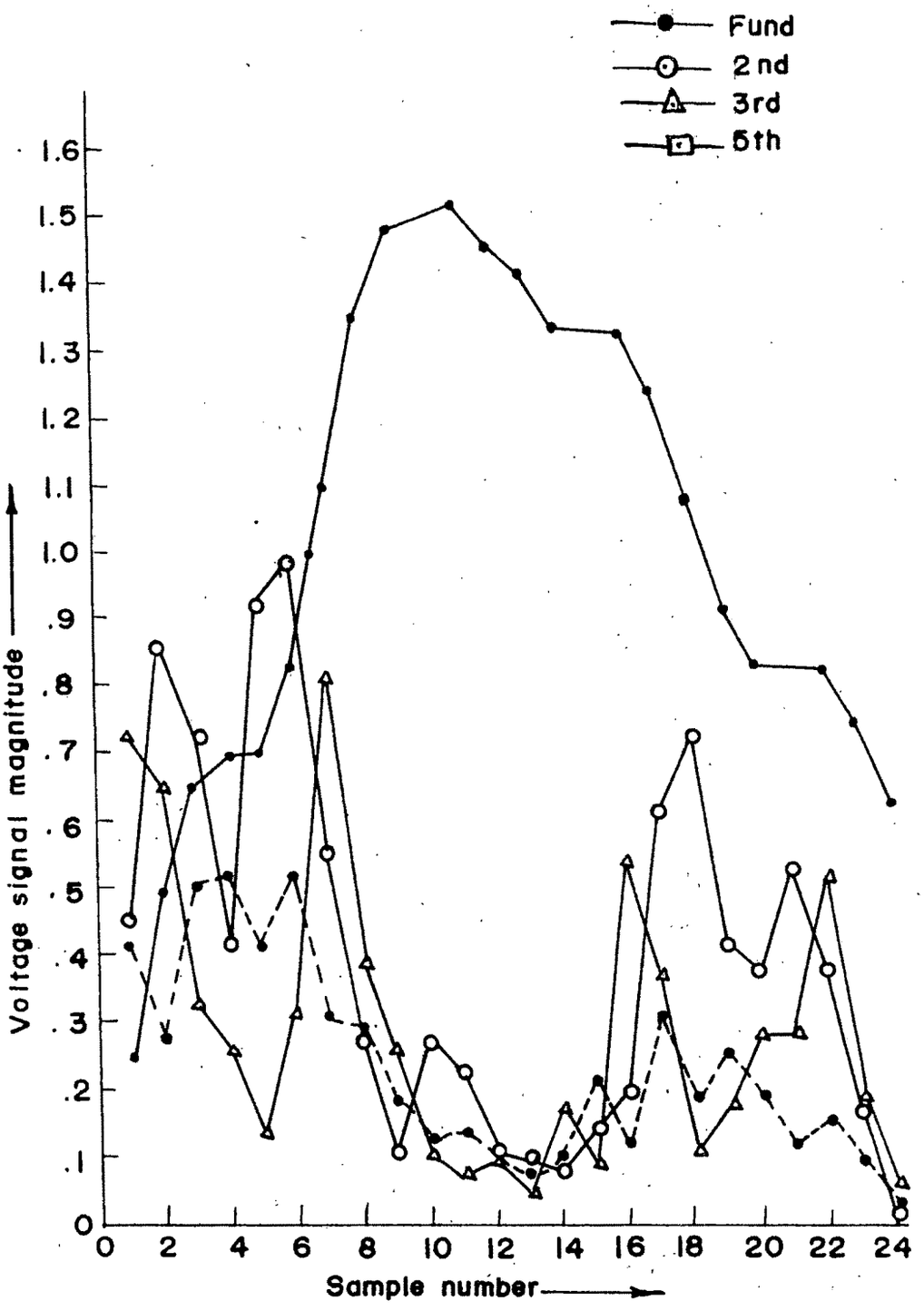

Fig. 4.6 Estimation of harmonics of voltage in an electrical transmission network using spectral observer

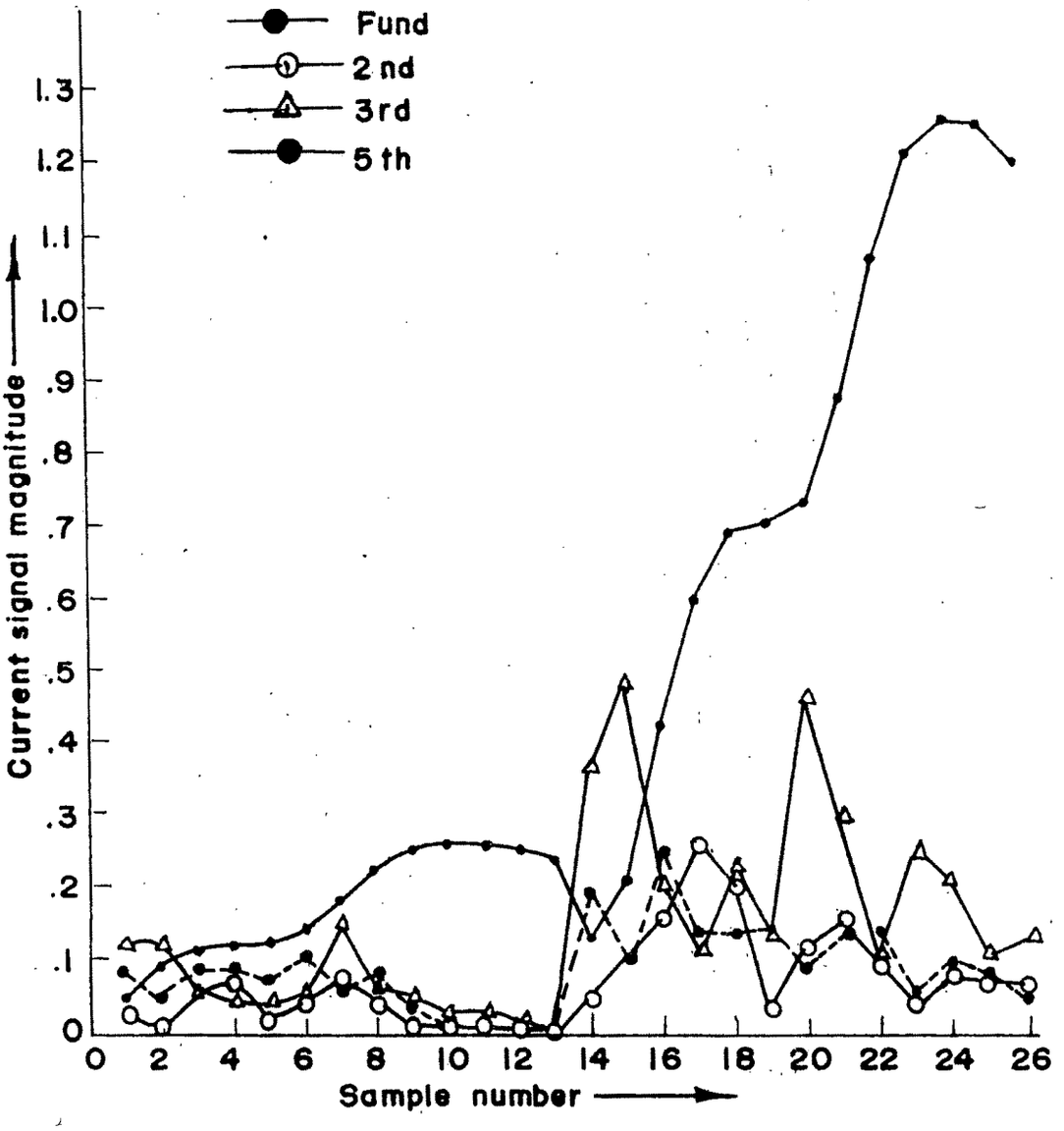

Fig. 4.7 Estimation of harmonics of currents in an electrical transmission network using spectral observer

4.5. ENERGY ESTIMATION BY AUTOCORRELATION

The energy of the current signal of the transformer is obtained by using an autocorrelation technique and implementing it on an LSI-11/23 microcomputer. This digital technique is fast and yields interesting information regarding the nature of the current rich in harmonics of different orders.

The autocorrelation of a signal corrupted with zero mean white Gaussian noise can be estimated by a fast digital method which involves additions only.

Let $x(t)$ be a zero mean stationary Gaussian process with a probability density function $f(x)$ given by

$$f(x) = \frac{1}{\sqrt{2x\ \sigma_x^2}}\, e^{-x^2/2\,\sigma_x^2} \tag{4.22}$$

and $Z(t) = \eta[x(t)]$ be a memoryless function of x.

Then

$$R_{zx}(\tau) = K\, R_{xx}(\tau) \tag{4.23}$$

where K is given by

$$K = \frac{1}{\sigma_x^2} \int_{-\infty}^{\infty} \eta(x)\, x\, f(x)dx \tag{4.24}$$

Now let $\eta(x)$ be chosen as

$$\eta(x) = \text{sign}(x) \cong \begin{cases} 1 & x > 0 \\ 0 & x = 0 \\ -1 & x < -1 \end{cases} \tag{4.25}$$

Then from (4.24) K is given by [53]

$$K = \frac{1}{\sigma_x^2} E|x| = \frac{1}{\sigma_x}\sqrt{\frac{2}{\pi}} \tag{4.26}$$

From (4.23) and (4.26)

$$R_{xx}(\tau) = \sqrt{\frac{\pi}{2}}\,\sigma_x\, R_{zx}(\tau) \tag{4.27}$$

and since $R_{xx}(0) = \sigma_x^2$

$$\sigma_x = \sqrt{\frac{\pi}{2}}\, R_{zx}(0) \tag{4.28}$$

From (4.27) and (4.28)

$$R_{xx}(\tau) = \frac{\pi}{2} R_{zx}(0)\, R_{zx}(\tau) \tag{4.29}$$

$R_{zx}(j)$ can be estimated by [54]. (Unit time sampling presumed)

$$\hat{R}_{zx}(j) = \frac{1}{n}\sum_{i=1}^{n} x(i)\, z(i + j)$$

$$= \frac{1}{n}\sum_{i=1}^{n} x(i)\, \text{sign}[x(i + j)] \tag{4.30}$$

where n is any number.

Hence, from (4.29) and (4.30) with

$$\hat{R}_{zx}(0) = \frac{1}{n} \sum_{i=1}^{n} |x(i)| R_{xx}(j)$$

then $\hat{R}_{xx}(j)$ can be estimated by

$$R_{xx}(j) = C_n \sum_{i=1}^{n} x(i) \text{ sign}[x(i+j)] \tag{4.31}$$

where

$$C_n = \frac{\pi}{2n^2} \sum_{i=1}^{n} |x(i)| \tag{4.32}$$

The autocorrelation is given by $R_{xx}(j)/C_n$.

From the above it is clear that this method is quite attractive because C_n needs to be computed only once and

$$\sum_{i=1}^{n} x(i) \text{ sign}[x(i+j)]$$

can be computed by addition only. Moreover, the shape of the autocorrelation can be computed by addition only.

From Figs. 4.8 and 4.9 it is seen that the energy content of the inrush current is much higher compared to the fault currents. Also it is found that in case of fault currents the autocorrelation function exhibits change in phase showing a kind of periodicity. These informations can be stored in a microcomputer memory for the protection of transformers during inrush and fault conditions.

4.6. CONCLUSIONS

This chapter presents two new recursive algorithms for estimating the harmonic contents of a signal usual in

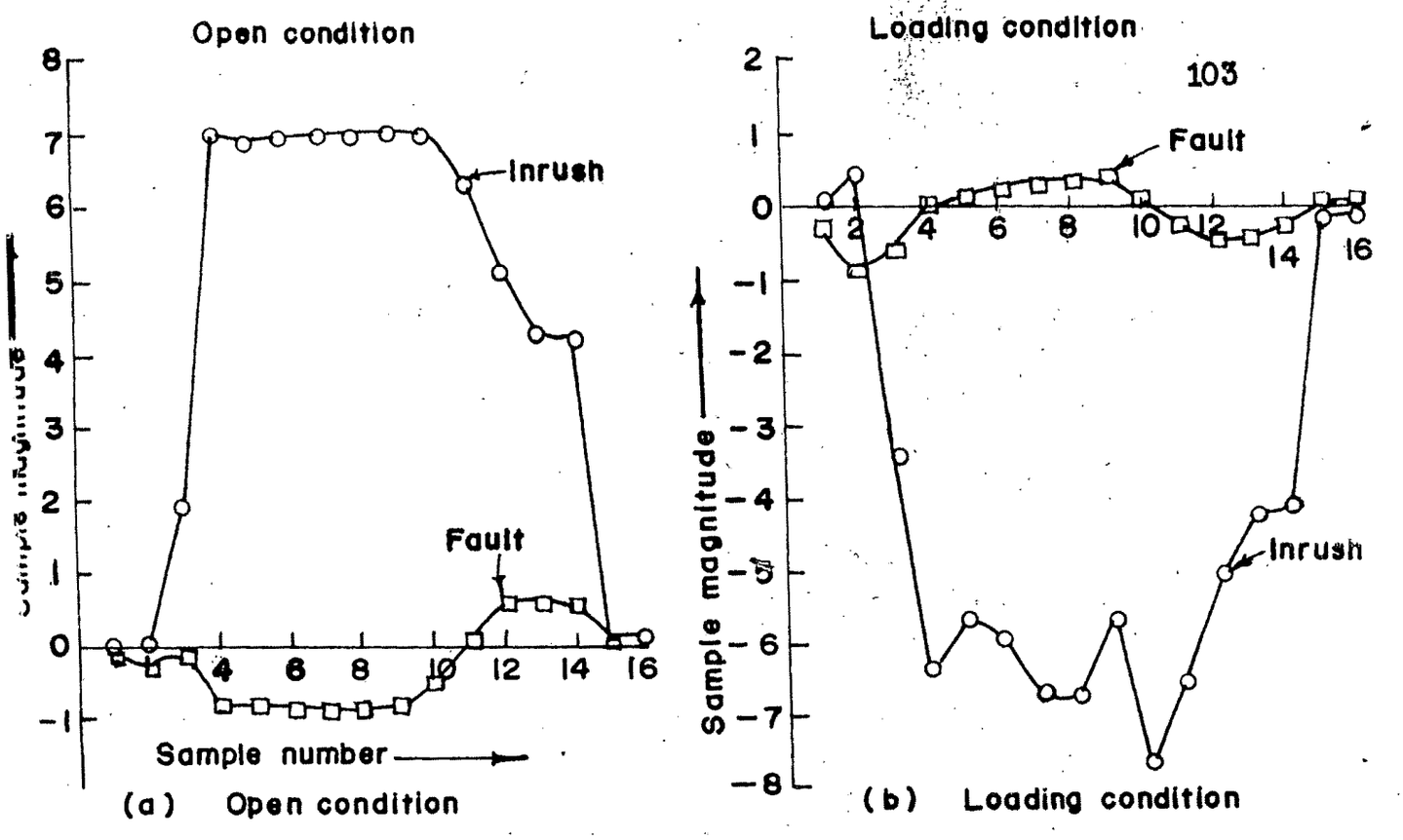

Fig. 4.8 Estimation of autocorrelation for magnetizing inrush currents in transformer

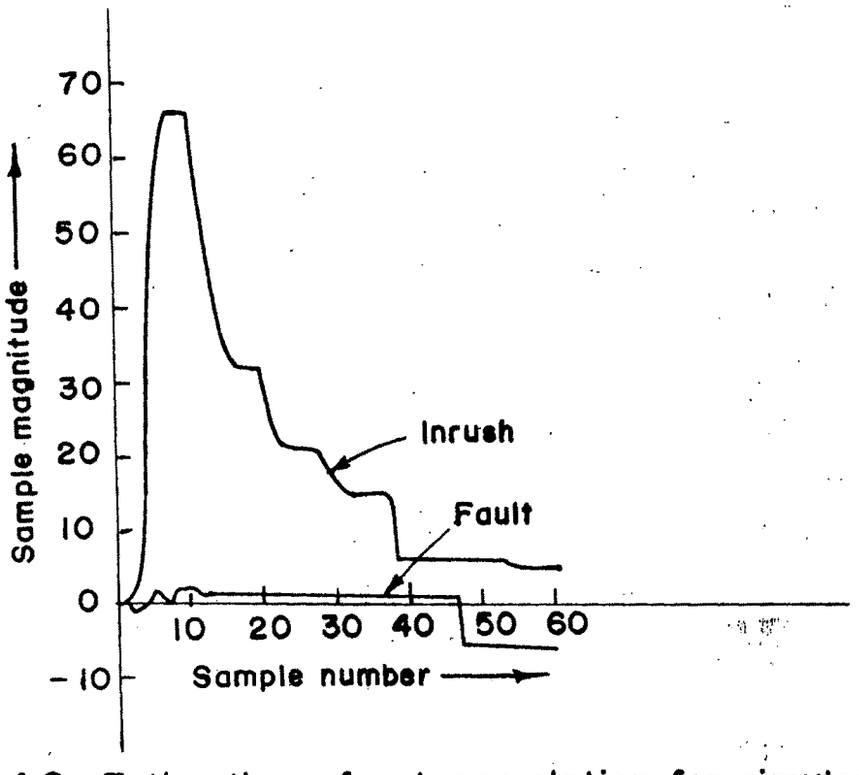

Fig. 4.9 Estimation of autocorrelation for simulated currents

electrical and electronic systems. The signal model is taken to be a general one and comprises a decaying d.c. component and several harmonic components. The algorithms have been tested in off-line and real-time conditions using an LSI-11/23 microcomputer system. They yield accurate results within 3/4 of a cycle based on 50 Hz waveform.

The estimated harmonics can be used for loss calculation and for digital instrumentation schemes. Further autocorrelation of the harmonic rich current signals produce interesting information during fault and inrush conditions in transformer.